Single-photon detection by rod cells of the retina

F. Rieke

*Department of Physiology and Biophysics, University of Washington,
Seattle, Washington 98195*

D. A. Baylor

Department of Neurobiology, Stanford University, Stanford, California 94305

At low light levels, the visual system detects and counts photon absorptions with a reliability close to limits set by statistical fluctuations in the number of absorbed photons. Thus the rod photoreceptors that provide the input signals to the dark-adapted visual system act as nearly perfect photon counters. This elegant performance is possible because light detection in the rods satisfies four functional requirements: high quantum efficiency, sufficient amplification to produce a measurable response, low dark noise, and low trial-to-trial variability in the elementary response. The rod meets these requirements using biochemical reactions rather than the solid-state reactions of silicon detectors, yet its performance equals or exceeds that of man-made detectors in several ways. [S0034-6861(98)00903-9]

CONTENTS

I. INTRODUCTION

On a dark night our visual system analyzes the signals provided by the eye's 100 million rod photoreceptor cells, each of which is capable of detecting the absorption of a single photon. The rod photoreceptors accomplish this feat with remarkable prowess. Incident photons within a broad band of wavelengths are absorbed with a probability approaching 0.5, and absorbed photons produce detectable output signals with an efficiency of about 0.6. The dark noise of rods is low, so that the single-photon response stands out clearly from the noise background. Furthermore, the responses to individual photons are reproducible, allowing the number of photons absorbed to be encoded unambiguously. Finally, rods are highly miniaturized — only a few micrometers in diameter — and contain their own power supply. Evidently these biological photon counters, built of protein, lipid, carbohydrate, and water, suffer little in comparison with man-made devices.

The rods are one of two types of photoreceptor cell comprising the transducing or input elements of the retina, a sheetlike outpost of the brain lining the inside of the back of the eye [Fig. 1(a)]. The photoreceptors convert incident light, imaged onto them by the eye's lens, into electrical signals. These signals are processed by other cells in the retina [Fig. 1(b)] and then sent to the brain, where interpretation of them produces visual images. Thus the spatial and temporal resolution of vision, as well as its absolute sensitivity, cannot exceed those of the input signals generated by the photoreceptor array. We see over an enormous range of light intensity, from photon fluxes of less than 10^{-2} photons $\mu m^{-2} sec^{-1}$ (starlight) to greater than 10^8 photons $\mu m^{-2} sec^{-1}$ (bright sunlight). The job of transducing light over this intensity range is divided between the two types of photoreceptor cell, which have very different sensitivities. The cone photoreceptors mediate vision over the upper 7–8 log units of the range. They mediate color vision and provide better temporal and spatial resolution. The rod photoreceptors mediate vision over the lower part of the intensity range. While they provide no color information and have poorer temporal and spatial resolution than the cones, the rods excel at detecting dim lights. It is the rods and their function that form the focus of this review.

Over much of the intensity range of rod vision, photons impinge on an individual rod at a rate of no more than a few per second. Thus good rod vision requires efficient, accurate photon counting, which in turn has several prerequisites: (1) a large fraction of the photons incident on the cell must be absorbed, and a captured photon must more often than not activate the molecule that absorbs it; (2) the energy of an absorbed photon must be amplified to produce a sizable electrical signal; (3) the electrical dark noise must be kept low so that it does not swamp the elementary response; and (4) the elementary response must have constant size and shape so that one photon can be distinguished reliably from zero and two. We shall discuss how the rod meets these requirements and compare its performance with that of man-made detectors such as photomultiplier tubes and charge-coupled devices.

II. EVIDENCE THAT RODS CAN DETECT A SINGLE PHOTON

The first indications that rod photoreceptors can detect the absorption of a small number of photons came
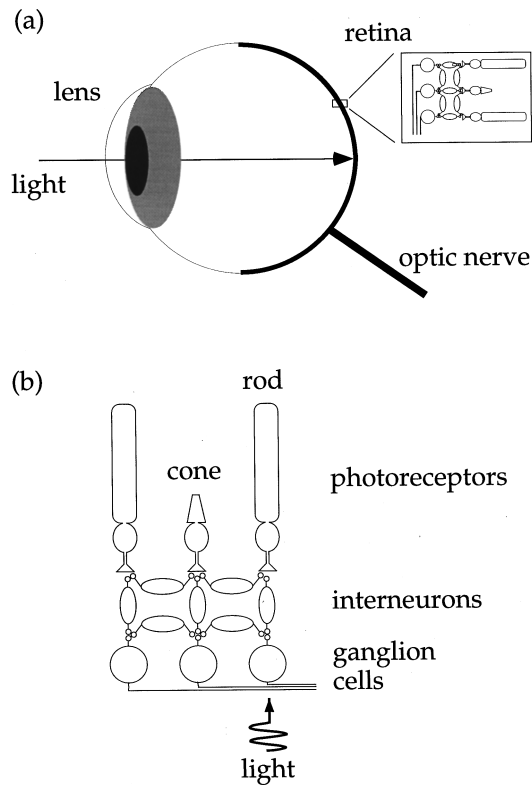
FIG. 1. Eye, lens, and retina. (a) Schematic of eye and retina. The retina is a thin layer of tissue lining the back of the eye. Light incident on the front of the eye is imaged onto the retina by a lens. The retina converts this light pattern into electrical activity and sends its output signals down the optic nerve to the brain. (b) Schematic of retina. The rod and cone photoreceptors are the transduction elements of the retina. Light passing through the retina is absorbed by the rods and cones and converted into electrical signals. The rods are exquisitely sensitive to dim lights, while the cones mediate vision at higher light levels and are responsible for color vision. The ganglion cells form the output elements of the retina. The interneurons between the photoreceptors and ganglion cells perform the initial steps in visual signal processing, including spatial and temporal filtering and amplification.

from behavioral measurements. In the early 1900s Lorentz realized that a just detectable flash of light delivered fewer than 100 photons to the front of the eye (see Bouman, 1961). The number of photons absorbed by an individual rod was significantly less than 100 because of internal scatter and absorption and because the flash fell on many photoreceptors. The implication of Lorentz's observation is that a rod can detect a few absorbed photons, perhaps even one.

Conclusive evidence that a rod can detect a single photon came independently from experiments by Hecht, Shlaer, and Pirenne (1942) and van der Velden (1946). These experiments made use of the statistics of photon absorption rather than unreliable estimates of the fraction of incident photons absorbed by the rods. Photons from a conventional light source arrive at the rod in a Poisson stream, and thus are absorbed in accordance with Poisson statistics. The notion that a rod can detect a
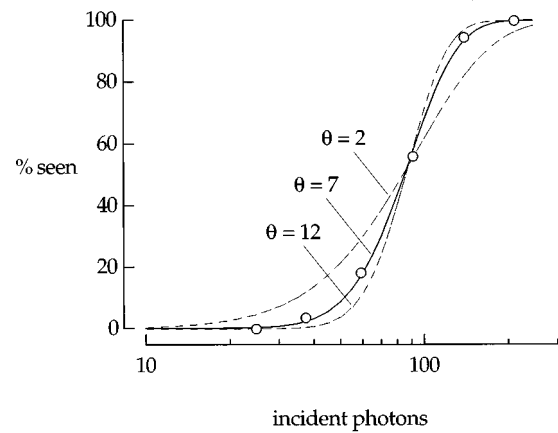

FIG. 2. Analysis of frequency of seeing experiment. The open symbols are measurements from a single human observer of the probability of seeing a flash plotted against the logarithm of the number of photons incident on the front of the eye for several flash strengths. These experimental measurements are compared to calculations from Eq. (2) for thresholds of 2, 7, and 12 photons. Each of the calculated curves has been shifted along the log intensity axis by varying the constant α which accounts for the fraction of incident photons producing a response in the rods. In this way the observer's threshold for detection can be measured independently of α (see text). Adapted from Hecht, Shlaer, and Pirenne (1942).

single photon was tested by comparing the statistics of the observed responses with expectations from Poisson statistics, as described below. A dark-adapted human observer was presented with a series of dim flashes and asked to report each time a flash was seen. The probability of seeing the flash was measured as a function of flash strength, producing a "frequency of seeing" curve such as that shown in Fig. 2, where the percent of the flashes that were seen is plotted against the logarithm of the flash strength. The transition between flashes that were seldom seen and those that were nearly always seen occurred over a considerable range of flash strengths. Hecht, Shlaer, and Pirenne and van der Velden attributed this gradual transition to Poisson fluctuations in the number of photons absorbed at a nominally fixed flash strength; thus dim lights occasionally produced enough absorptions to be seen, and bright lights sometimes produced too few. The smooth curves in Fig. 2 were calculated assuming that only flashes producing at least a threshold number of photon absorptions, θ, were seen; in this case the probability of seeing, p_{see}, is simply the probability that θ or more photon absorptions occur. This probability is given by the cumulative Poisson series

$$p_{see} = \sum_{n=\theta}^{\infty} \frac{\exp(-a)}{n!} a^n. \tag{1}$$

The mean number of photons absorbed per flash, a, is related to the flash strength I by $a = \alpha I$, where the proportionality factor α accounts for absorption and scatter prior to the rods. Equation (1) can then be rewritten as

$$p_{\text{see}} = \sum_{n=\theta}^{\infty} \frac{\exp(-\alpha I)}{n!}(\alpha I)^n. \tag{2}$$

When p_{see} is plotted against $\ln I$, the shape of the curve depends on the threshold θ but not on α. Thus Eq. (2) can be used to determine the number of photon absorptions required for detection without an accurate estimate of α (see Fig. 2). From this analysis Hecht, Shlaer, and Pirenne concluded that the dark-adapted human visual system can detect the absorption of 5–7 photons. As these photons were incident on an area of the retina containing 500 rods, individual rods must have detected the absorption of a single photon.

From a similar analysis, van der Velden (1946) concluded that the observer's detection threshold was two absorbed photons. Van der Velden, however, allowed a higher rate of false positive responses — reports that a flash was seen when none was given. These false positives arise when noise within the visual system becomes sufficiently large to generate the false perception of a flash. To suppress these responses, the observer's threshold must be high compared to the noise, as in Hecht, Shlaer, and Pirenne's experiments. Conversely, the higher false positive rate in van der Velden's experiments allowed a lower detection threshold.

Barlow (1956) suggested that the noise producing the false positive responses was produced by thermal noise in the retina itself — a "dark light" which was indistinguishable from real input signals. Sakitt (1972) pursued this idea by testing the hypothesis that the visual system can count photonlike events, some generated by photon absorption and others by internal noise. Sakitt asked her observers to rate the strength of each and every applied flash on a scale of 0–6 rather than indicating only whether the flash was seen. She then compared the statistics of each rating with expectations from Poisson statistics and found she could describe this set of data if the visual system literally counted photon absorptions beginning at one or two with a reliability limited by occasional photonlike noise events.

These behavioral experiments provide strong evidence that individual rods can detect the absorption of a single photon. Sakitt's work suggests further that the rods produce signals that allow neurons in the brain to discriminate between 1, 2, and 3 absorbed photons, and her experiments give an estimate of the rate of photonlike noise events that limit the reliability of this discrimination. Next we turn to measurements of the signal and noise in individual rods, with the aim of understanding the biophysical basis of their remarkable sensitivity.

III. PHOTORECEPTOR DARK CURRENT AND LIGHT RESPONSES

How does a rod signal the absorption of a photon? A rod that has been isolated from the salamander retina is shown in Fig. 3(a). The cell's surface membrane separates watery salt solutions inside and outside the cell. The predominant cation in the external solution is Na^+, while that in the internal solution is K^+. Light is con-
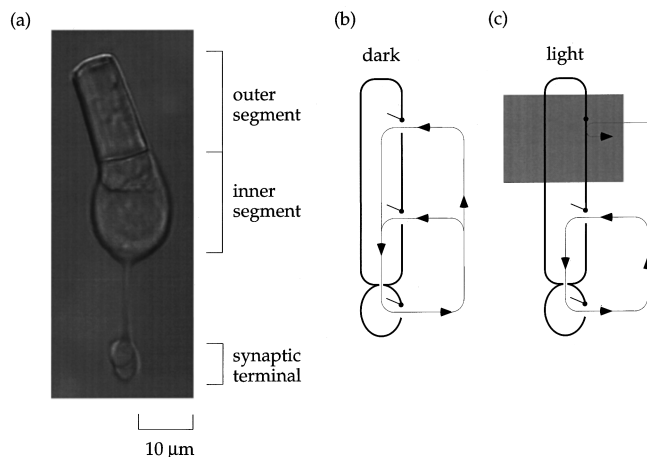

FIG. 3. Rod photoreceptor, dark current, and light response. (a) Isolated rod photoreceptor from the salamander retina. The salt solutions inside and outside the cell are separated by the lipid-bilayer membrane defining the cell's surface. The cell has several specialized regions. The outer segment transduces incident light into an electrical signal. The inner segment carries out many functions necessary to keep the cell alive, including generating the energy required for transduction in the outer segment. The synaptic terminal transmits the light responses to other cells in the retina, informing them about the amount of light falling on the outer segment. (b) Schematic of dark current. In darkness Na^+ ions enter the outer segment through channels in the surface membrane. The current loop is completed by the outward movement of K^+ ions from channels in the inner segment. The inner segment also expends energy to pump Na^+ out of the cell and K^+ into the cell and thus maintain their concentration gradients. In darkness this circulating current produces a voltage difference of about -40 mV between the inside and outside of the cell. (c) When the cell is exposed to light, some of the channels in the outer segment close and the circulating current decreases. The decrease in current causes a change in the voltage across the cell membrane which is communicated to second-order cells by changing the rate of release of a chemical transmitter from the synaptic terminal.

verted into an electrical signal in a specialized cylindrical part of the cell called the outer segment [see Fig. 3(a)]. In darkness a steady current enters the outer segment (Hagins, Penn, and Yoshikami, 1970). This current is carried mainly by Na^+ ions, which flow down their electrochemical gradient through "channels" — aqueous pores of atomic dimension in the surface membrane of the outer segment [Fig. 3(b)]. The current loop is completed by the outward flow of K^+ ions through channels of a different type in the inner segment of the cell. The inner segment expends energy to pump Na^+ out of the cell and replace it with K^+, thus maintaining the concentration gradients of Na^+ and K^+ required to sustain the dark current.

In darkness, the circulating current, electromotive forces across the cell membrane, and resistance of the membrane set a voltage difference of about -40 mV between the inside and outside of the cell. At this voltage a chemical transmitter is continuously released from the
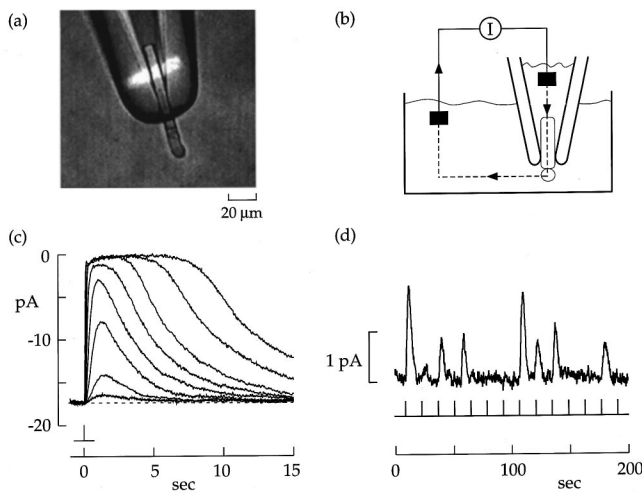
FIG. 4. Suction electrode recording of light-sensitive current. (a) Isolated toad rod, which has been drawn by suction into a tight-fitting glass electrode. The electrode collects the current entering the outer segment and allows changes in this current to be measured. The cell is viewed under infrared light (>850 nm) and stimulated with 500-nm light. (b) Current path in suction electrode recording. As is the case without the suction electrode, current carried by the movement of ions in solution flows into the outer segment and out of the inner segment. The suction electrode, however, provides a resistive barrier which prevents the current loop from being completed in the solution just outside the cell; instead current flows through an electrode placed in the bath, through a current-measuring amplifier, and into the suction electrode through another electrode. Thus changes in the outer-segment current can be directly measured. (c) Family of current changes to a brief flash recorded as in (a); the flash was given at $t=0$, as indicated by the timing bar. Averaged responses (4–5 trials) have been superimposed. The smallest response is to a flash producing an average of about one photon absorption; each successive flash is four times brighter. The flat tops of the responses to the brightest flashes are caused by closure of all the channels in the outer-segment membrane. (d) Current responses to repeated presentations of a dim, fixed flash given at the times indicated. The individual responses to this dim flash are quantized, corresponding to the effective absorption of 0, 1, or 2 photons.

cell's synaptic terminal [see Fig. 3(a)], a part of the cell specialized for communicating the rod signals to other cells in the retina. Light incident on the outer segment activates the photopigment rhodopsin, leading to closure of some of the channels in the outer segment and a decrease in the circulating current [Fig. 3(c)]. The reduction in current causes a change in the voltage across the rod's surface membrane. This voltage change quickly spreads to the synaptic terminal, where it alters the rate of release of chemical transmitter, thus informing other neurons in the retina about the amount of light falling on the outer segment.

The light-sensitive current can be recorded by drawing the outer segment into a tight-fitting glass electrode filled with the same solution bathing the outside of the cell [Fig. 4(a)]. The rod continues to operate as before, but the electrode collects the current flowing into the outer segment and allows light-evoked changes in the current to be monitored. Figure 4(b) shows the path of the electrical current for this recording configuration. Figure 4(c) shows superimposed responses to a series of brief light flashes recorded from a toad rod; each trace is the average of 4–5 individual responses. Prior to the flash there was an inward current of about 18 pA which decreased transiently in response to the flash. The smallest response was evoked by a flash producing an average of about one absorbed photon per trial and each successive flash was four times brighter. The brightest flashes closed all the channels in the outer segment membrane and completely shut off the current for several seconds. Dim flashes produced responses that rose slowly and lasted about 5 seconds. The sluggishness is due in part to the low temperature at which amphibian rods operate (20 °C in this experiment), but even in mammalian rods at 37 °C the dim flash response lasts 300 msec. The responses shorten considerably in the presence of steady background light, and cone photoreceptors generate much briefer light responses than rods. Because the kinetics of the photoreceptor responses limit the temporal sensitivity of the visual system, changes in the response kinetics can be demonstrated by observing the temporal frequency at which a sinusoidally modulated light appears constant rather than time varying. This "flicker-fusion" frequency is 3 Hz for dark-adapted human rod vision, but increases to 10 Hz for rod vision in the presence of steady light and rises to 50–60 Hz for cone vision in bright background light (Hecht and Verrijp, 1933).

The largest responses in Fig. 4(c) are like those our rods would generate in response to an intense camera flash in the middle of the night. Most of rod vision involves responses to much dimmer lights, such as those producing the very smallest responses in Fig. 4(c). The individual responses to these dim flashes are quantized, corresponding to the effective absorption of 0, 1, or 2 photons [Fig. 4(d)]. Indeed the number of responses in each group can be explained by the Poisson statistics of photon absorption (see Sec. VI). The responses to these very dim flashes exhibit two properties that are critical for reliable photon counting [Fig. 4(d)]: (1) the baseline is relatively stable so that the light responses can be clearly resolved (see Sec. V); and (2) the individual single-photon responses have reproducible amplitudes and shapes, allowing 1 absorbed photon to be clearly distinguished from 0 and 2 (see Sec. VI).

Good photon detection also requires that the rods harvest incident photons avidly and convert them into electrical signals with high efficiency. A blue-green photon traveling along the long axis of a 20 μm long human rod outer segment has a 50% chance of being absorbed. This high probability results from the very high density of rhodopsin molecules in the outer segment as well as the fact that the rhodopsin molecule itself absorbs very strongly. Furthermore, photon absorption activates the rhodopsin molecule (see below) and triggers an electrical response with a probability of 2/3.

IV. PHOTOTRANSDUCTION CASCADE

Thus far we have treated the rod outer segment as a black box that converts incident photons to a change in current. To further investigate the biophysical mechanisms responsible for the rod's remarkable sensitivity to dim lights, we need to examine the steps that link photon absorption to the change in current [Fig. 5(b)]. These steps comprise an amplifying cascade within the outer segment. The amplification causes at least 10^6 cations to fail to enter the outer segment during the single-photon response (reviewed by Pugh and Lamb, 1993). Amplification is essential if activation of a single rhodopsin molecule by photon absorption is to produce a macroscopic electrical signal that can be transmitted to the rest of the visual system.

The current carried by Na^+ and Ca^{2+} ions flows into the outer segment through channels held open in darkness by the binding of a diffusible chemical messenger, cyclic guanosine monophosphate (cGMP; Fesenko, Kolesnikov, and Lyubarsky, 1985; reviewed by Yau and Baylor, 1989); [see Fig. 5(b)]. The channels react in milliseconds to a change in the cGMP concentration (Karpen *et al.*, 1988) and thus, on the time scale of the flash response, can be thought of as instantaneous cGMP detectors whose output is the membrane current. A single channel can bind several cGMP molecules, and the dependence of the current I on the cGMP concentration G is described by (Yau and Baylor, 1989)

$$I = \frac{I_{max}}{1 + (K_{1/2}/G)^3} \approx kG^3,$$ (3)

where k is a proportionality constant, $K_{1/2}$ is the cGMP concentration at which the current is half maximal, and I_{max} is the maximal current. The approximation is valid for $G \ll K_{1/2}$, as is the case when the rod is operating normally. During the light response the cGMP concentration falls, some of the channels close, and the current decreases. Subsequent restoration of the cGMP concentration to its dark value terminates the light response. Thus light responses such as those in Fig. 4 are direct consequences of changes in the internal cGMP concentration. How then does photon absorption change the cGMP concentration?

When rhodopsin absorbs a photon its structure changes, converting it into a form that acts as a catalyst. In the catalytically active state, rhodopsin repeatedly activates copies of the protein transducin by colliding with it as both species diffuse laterally on one of the membrane discs inside the outer segment [Fig. 5(a),5(b)]. This amplifying process occurs at a rate close to the limit imposed by the rate of diffusional encounters (Pugh and Lamb, 1993); at least 1000 active transducins are produced within one second by a single active rhodopsin (Vuong, Chabre, and Stryer, 1984). Activated transducin rapidly activates another molecule associated with the disc membranes, cGMP phosphodiesterase (PDE) [see Fig. 5(b)]. This interaction does not involve amplification, but each PDE molecule destroys at least 50 cGMP molecules during its active lifetime. Destruction of
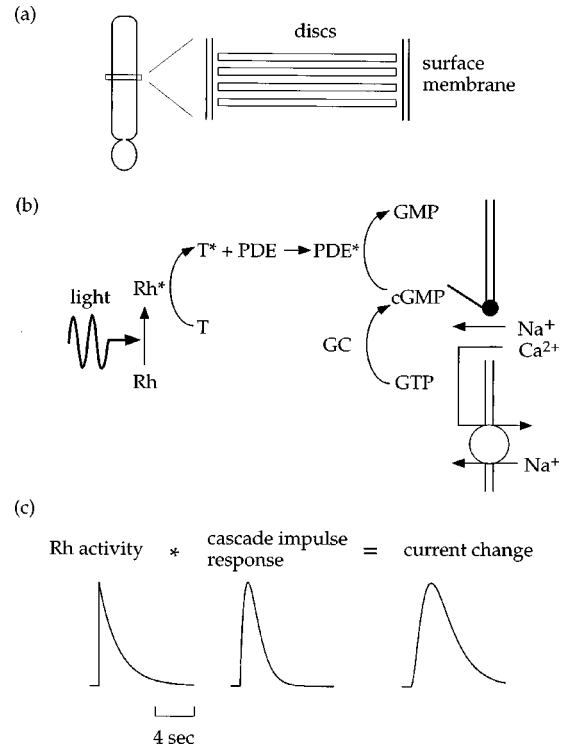

FIG. 5. Phototransduction cascade. (a) Outer-segment discs. A toad rod contains about 2000 membrane discs separated by about 30 nm; the initial steps of the phototransduction process occur as different molecular species diffuse and collide on the disc surface. (b) Schematic of transduction cascade. The light-sensitive current is carried by Na^+ and Ca^{2+} ions, which enter the outer segment through channels in the surface membrane. These channels are held open by the binding of cyclic guanosine monophosphate (cGMP). A decrease in cGMP in response to photon absorption permits some of the channels to close, reducing the current. The photopigment rhodopsin (Rh) is activated by photon absorption. Active rhodopsin catalyzes the activation of transducin (T), which in turn activates a cGMP phosphodiesterase (PDE). Activated PDE hydrolyzes cGMP, causing its concentration to fall. Recovery of the light response requires the restoration of the cGMP concentration. This is accomplished by guanylate cyclase (GC), which synthesizes cGMP from guanosine triphosphate (GTP). Ca^{2+} is removed from the outer segment by an exchange protein. (c) Contributions of rhodopsin activity and cascade to shape of dim flash response based on our recent experiments. For dim lights, the action of the transduction cascade can be approximated as a linear filter (see Sec. IV). The change in current produced by photon absorption can then be estimated by convolving the impulse response of this filter with the time course of rhodopsin's catalytic activity. Here we have described the time course of rhodopsin's activity as a declining exponential with a 2.5-sec time constant. The other parameters used in this calculation are the dark PDE activity $P_D = 0.1\ sec^{-1}$, the Ca^{2+} exchange time constant $\beta = 2\ sec^{-1}$, and the PDE decay rate $\phi = 2\ sec^{-1}$.

cGMP at the disc membrane is rapidly communicated to channels at the surface membrane by diffusion of cGMP. At the peak of the single-photon response, the lowered cGMP concentration causes several hundred channels to close. The final stage of amplification occurs

at the channels themselves, as the closure of one channel for a period of one second blocks the entry of more than 10^4 cations into the outer segment.

Rhodopsin continues to activate PDE at a high rate throughout its catalytic lifetime. The rate of change in PDE activity P produced by rhodopsin activity R can be described by

$$\frac{dP}{dt} = R(t) - \phi(P(t) - P_D), \tag{4}$$

where ϕ is the rate of decay of PDE activity and P_D is the PDE activity in the absence of active rhodopsin. For cGMP concentrations G within the normal physiological range, this PDE activity causes destruction of cGMP at a rate of PG. Synthesis of cGMP by guanylate cyclase [GC in Fig. 5(b)] replaces the destroyed cGMP and provides for the recovery of the flash response and dark current after the light-induced PDE activity has decayed. Thus the rate of change in the cGMP concentration is described by

$$\frac{dG}{dt} = \gamma - P(t)G(t), \tag{5}$$

where γ is the synthesis rate. Termination of the light response by cGMP synthesis is speeded by a feedback loop in which Ca^{2+} is a key dynamic messenger (Nakatani and Yau, 1988a; Matthews et al., 1988; reviewed by Koutalos and Yau, 1996). Ca^{2+} enters the outer segment through the cGMP-gated channels in the surface membrane and is removed by an exchange protein at a rate proportional to the internal Ca^{2+} concentration [Nakatani and Yau, 1988b; see Fig. 5(b)]. Thus the rate of change of the internal Ca^{2+} concentration C during the flash response can be approximated by

$$\frac{dC}{dt} \approx qI(t) - \beta C(t), \tag{6}$$

where q relates the current to Ca^{2+} entry and β is the rate constant for removal of Ca^{2+} from the outer segment. During the light response, Ca^{2+} influx decreases as channels close and the current decreases, but Ca^{2+} removal continues and the internal Ca^{2+} concentration

falls. This light-induced fall in Ca^{2+} increases the rate of synthesis of cGMP. The synthesis rate can be described by

$$\gamma = \frac{\gamma_{max}}{1 + (C/K)^2} \approx \gamma_{max}\left(\frac{K}{C}\right)^2, \tag{7}$$

where γ_{max} is the maximum synthesis rate and K describes its Ca^{2+} dependence. The approximation assumes $C \gg K$, which holds for Ca^{2+} concentrations close to those maintained in darkness.

Equations (3)–(7) describe the biochemical reactions that couple rhodopsin activity R to the membrane current I (see also Pugh and Lamb, 1993). Each of these biochemical reactions can be isolated, and the relevant parameters measured independently (for example, Koutalos, Nakatani, and Yau, 1995; Rieke and Baylor, 1996). Thus this approach provides a testable model for the transduction process based on the underlying biochemistry rather than an empirical description. Testing models such as the one described in Eqs. (3)–(7) is an important area of ongoing research.

A theoretical approximation to the dim flash response can be obtained from Eqs. (3)–(7) using a linear-response calculation (see Rieke and Baylor, 1996). First we separate the changes in PDE activity, cGMP concentration, and Ca^{2+} concentration from their respective dark values by writing the PDE activity as $P(t) = P_D + p(t)$, the cGMP concentration as $G(t) = G_D + g(t)$, and the Ca^{2+} concentration as $C(t) = C_D + c(t)$, where $p(t)$, $g(t)$, and $c(t)$ are the changes about the dark values P_D, G_D, and C_D. If p, g, and c are small compared to the dark values, Eqs. (3)–(7) can be expanded and only terms linear in p, g, and c retained. The resulting coupled linear differential equations can be solved using Fourier methods to approximate the rod's current response as a linear filter F convolved with the time course of rhodopsin's catalytic activity:

$$I(t) \approx I_D - 3kG_D^2 \int_0^t d\tau F(\tau)R(t-\tau), \tag{8}$$

where I_D is current in darkness. The Fourier transform of the filter F is given by

$$\tilde{F}(\omega) = \frac{G_D}{[\phi - i\omega][P_D + 6\beta^2 P_D/(\beta^2 + \omega^2) - i\omega(1 - 6\beta P_D/(\beta^2 + \omega^2))]}, \tag{9}$$

where $\tilde{F}(\omega) = \int dt \exp(i\omega t)F(t)$. This filter depends on two time scales described by the terms in square brackets in the denominator: (1) that governing the decay of PDE activity following rhodopsin shutoff; and (2) that governing the replenishment of the cGMP concentration by synthesis, including the feedback action of Ca^{2+}.

The kinetics of the dim flash response depend on the temporal filtering within the cascade, described by Eq.

(9), and the time course of rhodopsin's catalytic activity, which represents the input to the filter. A current question in phototransduction is whether rhodopsin's activity acts as a brief impulse initiating the flash response or whether it persists throughout much of the response. Our recent experiments suggest that rhodopsin's catalytic activity is relatively long lived; Fig. 5(c) provides an idea of how we think rhodopsin's activity and the filter-

ing by the cascade contribute to the shape of the dim flash response in a toad rod. The parameters used in the calculation are given in the figure legend.

V. DARK NOISE

The previous section summarizes our current understanding of how the rod transduces an absorbed photon into an electrical signal. The functional usefulness of these single-photon responses depends critically on the noise background in which they occur. This noise is generated by spontaneous activation of different elements of the transduction cascade and is important for several reasons: (1) it limits the ability of the rod and hence the visual system to detect dim lights (Barlow, 1956); (2) understanding the origin of the noise provides insights into the operation of the transduction cascade (Lamb, 1987; Rieke and Baylor, 1996); and (3) the frequency composition of the noise influences the appropriate strategy for temporal filtering of the rod responses at later stages of visual processing (Bialek and Owen, 1991).

Dark noise generated by the transduction cascade can be measured by recording the fluctuations in the current flowing into and out of the outer segment [Fig. 6(a)]. These current fluctuations consist of the cellular dark noise of interest as well as instrumental noise from the electronics and from thermal movement of ions across the resistance formed by the thin layer of solution between the cell and the suction electrode. The instrumental noise can be isolated by measuring the current fluctuations while the cell is exposed to a bright light that closes all the channels in the outer segment [Fig. 6(b)]. Assuming that the cellular and instrumental noise sources are independent and additive, they can be separated by subtracting the power spectrum of the current fluctuations measured in bright light from that of the current fluctuations measured in darkness [Fig. 6(c)].

There are two primary components of the cellular dark noise, each of which contributes about equally to the total variance of the dark current (Baylor, Matthews, and Yau, 1980). One component consists of occasional discrete events that resemble single-photon responses [arrows in Fig. 6(a)]. These events originate from thermal isomerization of rhodopsin and occur about once every 30 sec in a toad rod at 20 °C (Baylor, Matthews, and Yau, 1980) and about once every 90 sec in a mammalian rod at 37 °C (Baylor, Nunn, and Schnapf, 1984). The toad rod contains about 3×10^9 rhodopsin molecules, so each rhodopsin activates spontaneously only once every few thousand years; the mammalian rod contains about 10^8 rhodopsins, each of which activates spontaneously about once every 300 years at 37 °C. The second component of the dark noise is the continuous rumbling of the baseline in Fig. 6(a). This noise originates from spontaneous activation of PDE molecules (Rieke and Baylor, 1996), which causes the cGMP concentration to fluctuate. Although it seems an unnecessary evil, this spontaneous PDE activity may serve a useful purpose in providing a relatively brief
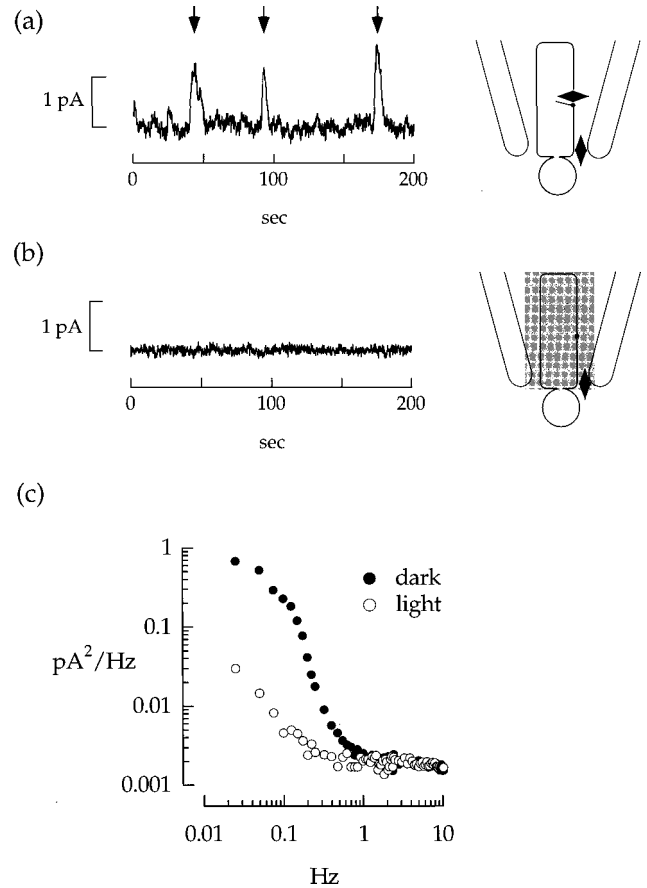

FIG. 6. Dark noise. (a) Fluctuations in the current collected by the suction electrode in darkness. These fluctuations come from two sources (schematic on right): cellular noise due to fluctuations in the current flowing into and out of the outer segment, and instrumental noise, including fluctuations in the current flowing across the seal of the outer segment into the suction electrode. The arrows mark three discrete photonlike noise events (see text). (b) Instrumental noise from the same cell as in (a). All the channels in the outer segment have been closed by exposing the cell to a bright light, leaving only instrumental noise. (c) Power spectra of the current fluctuations measured in (a) and (b).

light response. One of the rate constants in the linear approximation to the transduction cascade in Eq. (9) is the dark PDE activity P_D. Destruction of cGMP by spontaneous PDE activity must be balanced by synthesis to maintain the dark cGMP concentration and current. Recovery of the light response requires both the decay of light-activated PDE and the resynthesis of cGMP; the ongoing creation and destruction of cGMP in darkness speeds resynthesis, which causes faster recovery of the response. In the extreme case in which the synthesis rate is zero, the destroyed cGMP would never be replaced, and the flash response would be a step decrease in current.

Dark noise in the rod current appears to limit the sensitivity of the entire visual system, as the rate of spontaneous photonlike noise events estimated from behavioral measurements (see Sec. II) is within a factor of 2 of the rate of discrete noise events in the rod. This
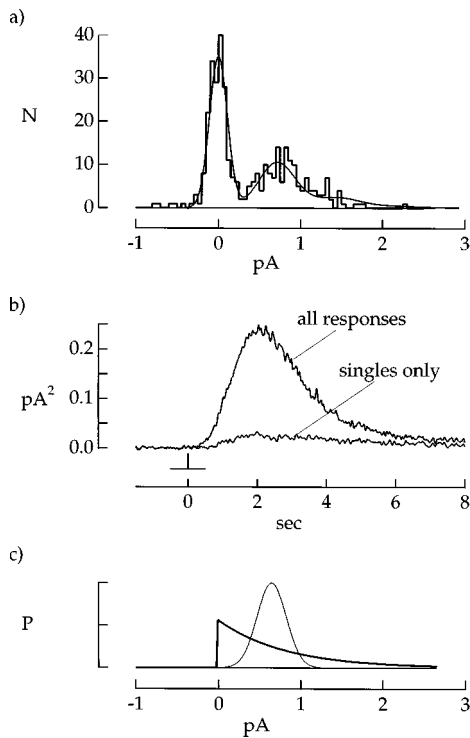
a)

b)

c)

FIG. 7. Reproducibility of the rod's elementary response. (a) Histogram of the response amplitudes from an experiment such as that in Fig. 4(d) in which 349 responses were collected. The peak centered around 0 pA is from trials in which no photons were effectively absorbed, and the peak around 0.6 pA from the single-photon responses. The smooth curve fitted to the experimental histogram is calculated assuming the noise in darkness and the noise in the single-photon response amplitude are independent and additive and that the number of photons absorbed per trial is described by Poisson statistics. This fit provides an estimate of the standard deviation and the mean of the elementary response amplitude; in this cell the mean was 3.9 times greater than the standard deviation. (b) Time-dependent ensemble variance of a series of dim flash responses and of single-photon responses alone. The variance in darkness has been subtracted in each case. The curve labeled "all responses" is calculated from all 349 responses contributing to the histogram in (a). The curve labeled "singles only" is calculated only for responses with amplitudes between 0.3 and 1.2 pA; most of these are responses to a single-absorbed photon. Thus the variance of the single-photon response is much smaller than the variance introduced by the Poisson statistics of photon absorption; this low variability of the elementary response allows for accurate photon counting. (c) Expected distribution of single-photon response amplitudes if rhodopsin's catalytic activity shuts off in a first-order, memoryless transition and the amplitude of the response is proportional to rhodopsin's lifetime. This exponential distribution is compared to the measured distribution of the single-photon response amplitudes from the experiment in (a).

agreement indicates that the neural circuitry processing the rod responses acts effectively noiselessly (Barlow, 1977). Indeed the dynamics of the initial step in the processing of the single-photon response can be predicted based on the rod signal and noise spectra and an optimal design argument (Bialek and Owen, 1991).

(a) SATURATION

(b) FEEDBACK
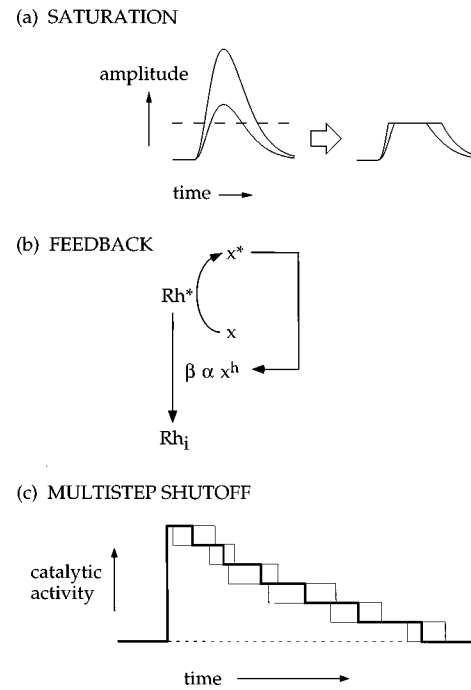

(c) MULTISTEP SHUTOFF

FIG. 8. Possible mechanisms responsible for the reproducibility of the rod's elementary response. (a) Saturation. Saturation of an element of the transduction cascade downstream of rhodopsin (e.g., closure of all channels) could reduce variability in the elementary response by making the current insensitive to fluctuations in the time course of rhodopsin's activity. (b) Feedback. A downstream activation product of rhodopsin could act as a feedback signal, causing rhodopsin to shut off once the elementary response had reached an appropriate amplitude. (c) Multistep rhodopsin deactivation. The rhodopsin molecule's catalytic activity might be reduced by a series of transitions, each of which reduced the activity by a small amount and occurred after a stochastic, first-order delay. In spite of variations in the timing of the transitions (e.g., three traces shown), the integrated catalytic activity would be more constant than that in the case where a single transition terminates rhodopsin's activity.

VI. REPRODUCIBILITY OF THE SINGLE-PHOTON RESPONSE

Reliable photon counting requires that the detector's responses to the same input vary little from trial to trial, so that the responses to each absorbed photon have a similar size and shape. The rod meets this requirement. If we repeatedly present a rod with a very dim flash of nominally fixed intensity, there are large intertrial fluctuations in the response due to variability in the number of absorbed photons, but there is little variability in the rod's response to a single absorbed photon. This reproducibility of the elementary response allows the rod to encode accurately the number of absorbed photons.

Reproducibility of the rod's elementary response can be demonstrated by presenting the rod with a series of dim flashes as in Fig. 4(d) and analyzing the statistics of the resulting responses. Figure 7(a) shows a simple statistical measure — a histogram of the maximum response amplitudes. The stepped curve is the experimen-

TABLE I. Comparison of light detection by rod photoreceptors, cone photoreceptors, photomultiplier tubes (PMT), and charge-coupled devices (CCD). Quantum efficiency refers to the probability that a photon incident on the surface of the retina or detector will produce a response. Dark noise refers to the equivalent rate of photonlike noise events. The integration time refers to the duration of a square pulse with area equal to that of the detector's single-photon response; in the case of the CCD the integration time refers to the time required to read the CCD and extract the photon count from a given pixel. Specifications for the CCD are from a Kodak KAF1400 chip, operating at $10\,^{\circ}$C and read out at 5 MHz. Specifications for the PMT are from a Hamamatsu photon-counting tube (R2371).

	Quantum eficiency	Dark noise	Integration time	Pixel area
Rod	0.25	$0.012\ \text{sec}^{-1}$	300 msec	$3\text{--}4\ \mu\text{m}^2$
Cone	0.05	$>1000\ \text{sec}^{-1}$	50 msec	$3\text{--}4\ \mu\text{m}^2$
PMT	0.25	$5\text{--}10\ \text{sec}^{-1}$	$<10^{-5}$ msec	$>10^8\ \mu\text{m}^2$
CCD	0.75	$1\ \text{sec}^{-1}$	100 msec	$\sim 60\ \mu\text{m}^2$

tal histogram with peaks corresponding to 0, 1, and 2 absorbed photons. The smooth theoretical curve was fitted to the measured histogram assuming that the noise in darkness and the noise in the elementary response are independent and additive and that the number of photons absorbed per trial is described by Poisson statistics. Such analysis shows that the mean amplitude of the elementary response is about five times greater than its standard deviation (Baylor, Lamb, and Yau, 1979).

The shape as well as the amplitude of the elementary response has low variability. Figure 7(b) shows the increase in the time-dependent ensemble variance produced by the flash (the ensemble variance measured in darkness has been subtracted). This variance includes contributions from Poisson fluctuations in the number of absorbed photons as well as variability in the elementary response. Variability in the elementary response itself can be isolated by considering only responses with peak amplitudes between 0.3 and 1.2 pA [the responses to a single absorbed photon in Fig. 7(a)]. Figure 7(b) also shows the residual variance of the elementary response. Throughout the time course of the elementary response, variability due to Poisson fluctuations in the number of absorbed photons is considerably larger than that due to fluctuations in the size and shape of the elementary response. This reproducibility of the elementary response allows the number of photons absorbed to be estimated accurately from the rod's response.

Reproducibility of the single-photon response is surprising because the response originates from a single activated molecule. We might expect large intertrial fluctuations in the duration of this molecule's activity, similar to the fluctuations observed in the lifetime of a single radioactive particle. For example, if rhodopsin's active lifetime were terminated by a first-order, memoryless transition, then the distribution of active lifetimes would be exponential. If the response amplitude were proportional to rhodopsin's lifetime, the amplitude dis-

tribution would also be exponential with a ratio of the standard deviation to the mean of 1 — quite different from the observed ratio of 1/5 [Fig. 7(c)]. Thus somehow the rod has avoided the fluctuations we expect from the stochastic shutoff of a single molecule.

What makes the elementary response reproducible? Apparently either the membrane current is insensitive to variability in rhodopsin's active lifetime or such variability is small. These possibilities are broken down as three potential mechanisms in Fig. 8. Our recent results indicate that reproducibility arises from low variability in rhodopsin's catalytic activity and suggest that this low variability is not due to a feedback pathway but may instead result from multiple steps in the shutoff of rhodopsin's catalytic activity [Fig. 8(c)]. The physical basis of these steps is not known.

VII. SUMMARY AND OPEN QUESTIONS

Rod photoreceptors detect and encode incident photons exceptionally well, providing highly sensitive input to the visual system at low light levels. They collect sparse photons with high efficiency, as more than 25% of the photons incident on the retina produce a rod response. They maintain a low dark noise, equivalent to a light producing one absorbed photon every 90 sec in a human rod. And they generate reproducible responses to each absorbed photon, allowing the number of photons absorbed to be accurately determined from the rod signals. In lights producing more than one absorbed photon per rod every 10–20 sec, Poisson fluctuations in the incident photons dominate the rod's internal noise, and the cell acts as a nearly perfect photon counter. The performance of a mammalian rod is compared with that of a cone photoreceptor, a photomultiplier tube (PMT) and a charge-coupled device (CCD) in Table I. Rods have lower dark noise and smaller pixel areas than the PMT and CCD, but the PMT's integration time is much shorter. Cones have a lower quantum efficiency and much larger dark noise than the rods, but a shorter integration time.

Although our understanding of visual transduction and signal processing has advanced rapidly during the past 15 years, several fundamental questions remain: (1) What mechanisms are responsible for the reproducibility of the rod's elementary response? (2) How are the rod's single-photon responses reliably transmitted to the rest of the visual system? (3) What is the molecular basis for the differences in kinetics, sensitivity, and dynamic range of rod and cone photoreceptors? The answers to these and related questions will deepen our understanding of the strategies and capabilities of biological detectors.

REFERENCES

Barlow, H. B., 1956, "Retinal noise and absolute threshold," J. Opt. Soc. Am. **46**, 634–639.

Barlow, H. B., 1977, in *Vertebrate Photoreception*, edited by H. B. Barlow and P. Fatt (Academic, London), pp. 337–351.

Baylor, D. A., T. D. Lamb, and K.-W. Yau, 1979, "Responses of retinal rods to single photons," J. Physiol. (London) **288**, 613–634.

Baylor, D. A., G. Matthews, and K.-W. Yau, 1980, "Two components of electrical dark noise in toad retinal rod outer segments," J. Physiol. (London) **309**, 591–621.

Baylor, D. A., B. J. Nunn, and J. L. Schnapf, 1984, "The photocurrent, noise and spectral sensitivity of rods of the monkey *Macaca fascicularis*," J. Physiol. (London) **357**, 575–607.

Bialek, W., and W. G. Owen, 1991, "Temporal filtering in retinal bipolar cells: Elements of an optimal computation," Biophys. J. **58**, 1227–1233.

Bouman, M. A., 1961, in *Sensory Communication*, edited by W. Rosenblith (MIT, Cambridge, MA), pp. 377–401.

Fesenko, E. E., S. S. Kolesnikov, and A. L. Lyubarsky, 1985, "Induction by cyclic GMP of cationic conductance in plasma membrane of retinal rod outer segment," Nature (London) **313**, 310–313.

Hagins, W. A., R. D. Penn, and S. Yoshikami, 1970, "Dark current and photocurrent in retinal rods," Biophys. J. **10**, 380–412.

Hecht, S., S. Shlaer, and M. Pirenne, 1942, "Energy, quanta and vision," J. Gen. Physiol. **25**, 819–840.

Hecht, S., and C. D. Verrijp, 1933, "Intermittent stimulation by light," J. Gen. Physiol. **17**, 251–268.

Karpen, J. W., A. L. Zimmerman, L. Stryer, and D. A. Baylor, 1988, "Gating kinetics of the cyclic-GMP-activated channel of retinal rods: flash photolysis and voltage-jump studies," Proc. Natl. Acad. Sci. USA **585**, 1287–1291.

Koutalos, Y., K. Nakatani, and K.-W. Yau, 1995, "The cGMP-phosphodiesterase and its contribution to sensitivity regulation in retinal rods," J. Gen. Physiol. **106**, 891–921.

Koutalos, Y., and K.-W. Yau, 1996, "Regulation of sensitivity in vertebrate rod photoreceptors by calcium," Trends Neurosci. **19**, 73–81.

Lamb, T. D., 1987, "Sources of noise in photoreceptor transduction," J. Opt. Soc. Am. A **4**, 2295–2300.

Matthews, H. R., R. L. W. Murphy, G. L. Fain, and T. D. Lamb, 1988, "Photoreceptor light adaptation is mediated by cytoplasmic calcium concentration," Nature (London) **334**, 67–69.

Nakatani, K., and K.-W. Yau, 1988a, "Calcium and light adaptation in retinal rods and cones," Nature (London) **334**, 69–71.

Nakatani, K., and K.-W. Yau, 1988b, "Calcium and magnesium fluxes across the plasma membrane of the toad rod outer segment," J. Physiol. (London) **395**, 695–729.

Pugh, E. N. Jr., and T. D. Lamb, 1993, "Amplification and kinetics of the activation steps in phototransduction," Biochim. Biophys. Acta **1141**, 111–149.

Rieke, F., and D. A. Baylor, 1996, "Molecular origin of continuous dark noise in rod photoreceptors," Biophys. J. **71**, 2553–2572.

Sakitt, B., 1972, "Counting every quantum," J. Physiol. (London) **223**, 131–150.

van der Velden, H. A., 1946, "The number of quanta necessary for the perception of light in the human eye," Ophthalmologica **111**, 321–331.

Vuong, T. M., M. Chabre, and L. Stryer, 1984, "Millisecond activation of transducin in the cyclic nucleotide cascade of vision," Nature (London) **311**, 659–661.

Yau, K.-W., and D. A. Baylor, 1989, "Cyclic GMP-activated conductance of retinal photoreceptor cells," Annu. Rev. Neurosci. **12**, 289–327.